System-Level Performance of Downlink NOMA for Future LTE Enhancements

Anass Benjebbour† Anxin Li‡ Yuya Saito† Yoshihisa Kishiyama† Atsushi Harada‡ Takehiro Nakamura†

†Radio Access Network Development Department, NTT DOCOMO, INC.
‡DOCOMO Beijing Communications Laboratories Co., Ltd.
anass@nttdocomo.co.jp

***Abstract*—This paper investigates the system-level performance of downlink non-orthogonal multiple access (NOMA) with power-domain user multiplexing at the transmitter side and successive interference canceller (SIC) on the receiver side. The goal is to clarify the performance gains of NOMA for future LTE (Long-Term Evolution) enhancements, taking into account design aspects related to the LTE radio interface such as, frequency-domain scheduling with adaptive modulation and coding (AMC), and NOMA specific functionalities such as error propagation of SIC receiver, multi-user pairing and transmit power allocation. In particular, a pre-defined user grouping and fixed per-group power allocation are proposed to reduce the overhead associated with power allocation signalling. Based on computer simulations, we show that for both wideband and subband scheduling and both low and high mobility scenarios, NOMA can still provide a hefty portion of its expected gains even with error propagation, and also when the proposed simplified user grouping and power allocation are used.**

Keywords*– *non-orthogonal multiple access, LTE, superposition, successive interference canceller, adaptive modulation and coding

I. INTRODUCTION

In order to continue to ensure the sustainability of 3GPP radio access technologies over the coming decade (LTE Release 13 and onwards), new solutions that can respond to future challenges must be identified and developed [1]. In the future, significant gains in capacity and quality of user experience (QoE) are required in view of the anticipated exponential increase in the volume of mobile traffic, e.g., beyond a 500 fold increase in the next decade. In cellular mobile communications, the design of radio access technology (RAT) is one important aspect in improving system capacity in a cost-effective manner. Radio access technologies are typically characterized by multiple access schemes, e.g., frequency division multiple access (FDMA), time division multiple access (TDMA), code division multiple access (CDMA), and orthogonal frequency-division multiple access (OFDMA), which provide the means for multiple users to access and share the system resources simultaneously. In the 3.9 and 4th generation (4G) mobile communication systems such as Long-Term Evolution (LTE) and LTE-Advanced [2,3], standardized by the 3rd Generation Partnership Project (3GPP), orthogonal multiple access (OMA) based on OFDMA or single carrier (SC)-FDMA was adopted. The orthogonal design of multiple access is a reasonable choice for achieving good system-level throughput performance in packet radio services with a simplified receiver design. However, in order to boost further the spectrum efficiency, more advanced receiver designs are required in order to mitigate intra-cell and/or inter-cell interference. In [4-7], we proposed a downlink non-orthogonal multiple access (NOMA) where multiple users are multiplexed in the power-domain at the transmitter side and multi-user signal separation is conducted at the receiver side based on successive interference cancellation (SIC). From an information-theoretical point of view, it is well-known that non-orthogonal user multiplexing using superposition coding at the transmitter and SIC at the receiver not only outperforms orthogonal multiplexing, but also is optimal in the sense of achieving the capacity region of the downlink broadcast channel [8]. In [9], the basic concept and benefits of NOMA as a candidate future multiple access are explained and discussed in detail. In [10, 11], initial system-level evaluation results of NOMA were discussed and investigated to demonstrate its potential gains in a low mobility scenario assuming no error propagation, exhaustive full search on candidate user pairs, and dynamic transmit power allocation.

The goal of this work is two-fold: The first is to clarify the gains of NOMA compared to OMA under more practical wide-area cellular system configurations with both wideband and subband frequency scheduling in both low mobility and high mobility environments; and the second is to clarify the degree of impact of error propagation of SIC receiver, multi-user power allocation and user grouping on the performance of NOMA. Specifically, NOMA is shown to provide 30 to 40% gains compared to OMA for both wideband and subband scheduling, and have good robustness to mobility as it mainly relies on receiver side channel state information (CSI) and processing. On the other hand, the effect of the error propagation owing to the successive cancellation of interference is shown negligibly small using a worst-case model which we used to emulate error propagation in the system-level simulations. In addition, a simplified user pairing on the basis of pre-defined thresholds and simplified transmit power allocation (TPA) with fixed power assignment ratio are proposed for practical usage with reduced scheduling complexity and downlink signalling overhead associated with dynamic power allocation. The performance of NOMA using proposed schemes is compared with that of NOMA using more advanced (exhaustive) schemes. It is shown that even with simplified TPA and pre-defined user grouping, a large portion of NOMA gains can be maintained.

The remainder of this paper is organized as follows. Section II describes the system model and the key functionalities utilized to introduce NOMA. Section III discusses the key aspects related to the design of the radio interface of NOMA. In section IV, after describing the employed system-level simulations, we provide and discuss the results of the system-level performance of NOMA in comparison to that of OMA. Finally, Section V concludes the paper.

II. DESCRIPTION OF NOMA WITH SIC

This section describes the system model and key functionalities utilized in NOMA for user multiplexing at the transmitter of the base station (BS) with SIC applied at the receiver of the user terminal (User Equipment (UE)). Throughout this paper, we assume a 1-by-2 single input multiple output (SIMO) system where the number of transmitter antennas at the BS is one ($N_t = 1$), while the number of receiver antennas at the UE is two ($N_r = 2$). There are K users per cell and the total transmit bandwidth, BW, is divided into S subbands, where the bandwidth of each subband is B ($BW = S \times B$). We assume that the multi-user scheduler selects m_s users from K then schedules a set of users, $U_s = \{i_s(1), i_s(2), ..., i_s(m_s)\}$, to subband s ($1 \leq s \leq S$), where $i_s(l)$ indicates the index of the l-th ($1 \leq l \leq m_s$) user scheduled

at subband s, and m_s denotes the number of users non-orthogonally multiplexed at subband s. For the sake of simplicity, hereafter the time index, t, and the subcarrier index, f, are omitted and the channel coefficients are indicated as constants within each subband.

A. Signal Model and Scheduling Signal-to-Interference Plus Noise Power Ratio Calculation

The transmit signal, x_s, at every subcarrier of subband s is a summation of the coded modulation symbol, $d_s(i_s(l))$, of the $i_s(l)$-th user. Thus, $d_s(i_s(l))$ of all m_s users are superposed in power-domain as

$$x_s = \sum_{l=1}^{m_s} \sqrt{p_s(i_s(l))}\, d_s(i_s(l)), \quad (1)$$

where $E[|d_s(i_s(l))|^2] = 1$ and $p_s(i_s(l))$ is the allocated transmit power to user $i_s(l)$ at subband s. The N_r dimensional received signal vector of user $i_s(l)$ at every subcarrier of subband s, $\boldsymbol{y}_s(i_s(l))$, is represented by

$$\boldsymbol{y}_s(i_s(l)) = \boldsymbol{h}_s(i_s(l))x_s + \boldsymbol{w}_s(i_s(l)), \quad (2)$$

where $\boldsymbol{h}_s(i_s(l))$ is the N_r-dimensional channel coefficient vector of user $i_s(l)$ at subband s, which includes distance dependent loss, shadowing loss, and instantaneous fading coefficients, and $\boldsymbol{w}_s(i_s(l))$ is the N_r-dimensional noise plus inter-cell interference vector of user $i_s(l)$ at subband s. Assuming that the receiver treats inter-cell interference as white noise, at the receiver maximal ratio combining (MRC) is applied to $\boldsymbol{y}_s(i_s(l))$ as follows:

$$\begin{aligned} \tilde{y}_s(i_s(l)) &= \boldsymbol{h}_s^{\boldsymbol{H}}(i_s(l))\boldsymbol{y}_s(i_s(l))/\|\boldsymbol{h}_s\| \\ &= \sqrt{G_s(i_s(l))}x_s + n_s(i_s(l)) \\ &= \sqrt{G_s(i_s(l))}\sum_{k=1}^{m_s}\sqrt{p_s(i_s(k))}\, d_s(i_s(k)) \\ &\quad + n_s(i_s(l)) \end{aligned} \quad (3)$$

where $G_s(i_s(l)) = \|\boldsymbol{h}_s(i_s(l))\|^2$ is the combining gain after MRC, while $n_s(i_s(l)) = \boldsymbol{h}_s^{\boldsymbol{H}}(i_s(l))\boldsymbol{w}_s(i_s(l))/\|\boldsymbol{h}_s\|$ is the noise plus inter-cell interference after MRC. The average power of $n_s(i_s(l))$ is denoted as $N_s(i_s(l)) = E[|n_s(i_s(l))|^2]$. In the following, we define the channel gain of user $i_s(l)$ at subband s as $G_s(i_s(l))/N_s(i_s(l))$. In addition, we assume that the total transmission power per subband of the BS is common to all subbands and equals to P. Thus, for each subband s, the sum power constraint is represented by

$$\sum_{l=1}^{m_s} p_s(i_s(l)) = P. \quad (4)$$

At the receiver, U_s being the scheduled user set at subband s and user $i_s(l)$, $j \in U_s$, the scheduling signal-to-interference plus noise power ratio (SINR) at the receiver of each user, $i_s(l)$, is derived as in (5). Assuming that the receiver of user $i_s(l)$, is able to cancel perfectly and successively the interference from other user(s) j with channel gain $G_s(j)/N_s(j)$ lower than $G_s(i_s(l))/N_s(i_s(l))$, the decoding and cancellation procedure, at the receiver of user $i_s(l)$, the SINR of user $i_s(l)$ at subband s, is represented as

$$SINR_s(i_s(l)|U_s) = \frac{G_s(i_s(l))p_s(i_s(l))}{\sum_{j\in U_s, \frac{G_s(i_s(l))}{N_s(i_s(l))} < \frac{G_s(j)}{N_s(j)}} G_s(i_s(l))p_s(j) + N_s(i_s(l))} \quad (5)$$

Note that the decoding and the successive cancellation order of signals from other users with higher channel gains are carried out in the order of the increasing channel gain. On the other hand, at the receiver of each user, $i_s(l)$, the received signal from other user(s) j with channel gain $G_s(j)/N_s(j)$ higher than $G_s(i_s(l))/N_s(i_s(l))$ is treated as noise, thus neither decoding nor cancellation of these users' signals is performed at the receiver of user $i_s(l)$. Figure 1 illustrates the structure of the SIC receiver for the case of 2 UEs (m_s =2), with UE 1 having higher channel gain, and thus being allocated lower transmission power, than UE 2.

B. Multi-user Scheduling and Candidate User Set Selection

In NOMA, the scheduler allocates more than one user for transmission for each subband. The scheduling metric adopted significantly affects the system capacity (measured by, for example, cell throughput) and fairness (measured by, for example, cell-edge user throughput). The proportional fairness (PF) scheduler [12] is known to achieve a good balance between system capacity and user fairness by maximizing proportional fairness, i.e., the product of the average user throughput among all users within a cell. In [13], the multiuser scheduling version of the PF scheduler is presented and an approximated version is derived. In the approximated version, among all candidate user sets, the PF scheduling metric maximizing candidate user set U_s is selected as follows:

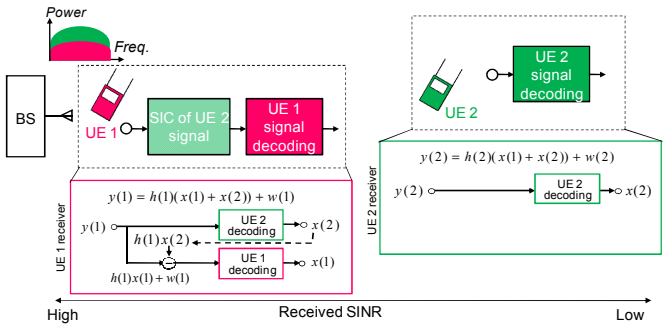

Fig. 1. Structure of SIC receiver (Case of 2-UE).

$$Q_s(U) = \sum_{k\in U}\left(\frac{R_s(k|U,t)}{L(k,t)}\right)$$
$$U_s = \max_U Q_s(U) \quad (7)$$

Term $Q_s(U)$ denotes the PF scheduling metric for candidate user set U, and it is given by the summation of the PF scheduling metric of all users in user set U. Term $R_s(k|U, t)$ is the instantaneous throughput of user k in subband s at time instance t (the time index of a subframe), whereas $L(k,t)$ is the average throughput of user k. When $t_c >> 1$, which is valid in this paper as t_c is set to 200, (7) provides a good approximation of the multiuser proportional fairness policy that maximizes the product of the average throughput of the K users.

III. Design Considerations for NOMA

A. User Scheduling and MCS Selection: Wideband vs. Subband

In LTE, the same channel coding rate (including rate matching) and data modulation scheme are assumed over all the subbands allocated to each single user, as the average SINR over all the subbands is used for MCS selection. However, for NOMA, such a mismatch between MCS adaptation subband unit (e.g., wideband) and power allocation subband unit (e.g., subband) does not allow to fully exploit NOMA gains [11]. Here, we explore NOMA performance gains with subband scheduling and subband MCS and compare it to NOMA with wideband scheduling and wideband MCS selection.

B. Modeling of error propagation for SIC receiver

In order to emulate error propagation of the SIC receiver in the system level simulations of NOMA, we assume a worst-case model. The model used is explained in Fig. 2 for the case of 2 UEs. At the receiver of UE1, where SIC is applied, the decoding of UE2 is performed first at stage 1. Based on the knowledge of the MCS assigned to UE2 and the received SINR, the BLER of the user decoded first (UE2) is obtained and decoding is attempted. Then, its replica signal is generated and subtracted from the received signal before the decoding of UE1 at stage 2. Thus, depending on the decoding result of UE2 (successful (OK) or unsuccessful (NG)) at stage 1, the signal used for the decoding of UE1 at stage 2 differs. To emulate this in system-level simulations, this would require complicated link-to-system mapping. To simplify, here we assume a worst-case model where the decoding of UE1 at stage 2 is always unsuccessful whenever the decoding of UE2 at stage 1 of the UE1 receiver is unsuccessful. Also, the HARQ process of the corresponding to UE1 transmission is terminated by emptying the

HARQ buffer and requesting a new transmission. Such a worst-case model is simple but provides us with a good estimation of the impact of error propagation on NOMA performance. This is because users with lower channel gains, as explained later, are allocated higher levels of transmit power than users with higher channel gains. Thus, their unsuccessful decoding at the receivers of users with higher channel gains (i.e., lower levels of transmit power) would cause high probability of error propagation to these users.

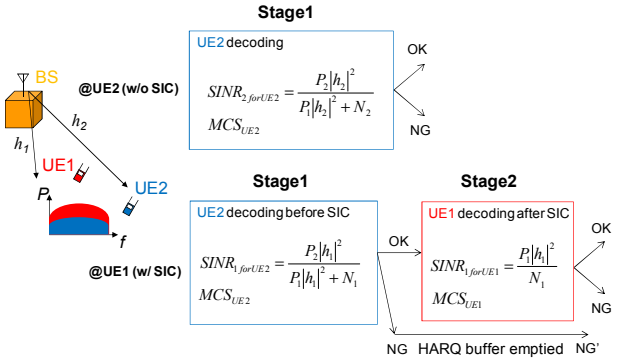

Fig. 2. Error propagation modeling.

With high temporal channel variations (e.g., channel gain of UE1 larger than that of UE2 @ feedback time but lower @ decoding time), more error propagation are expected to occur due to the failure to decode UE2 at UE1 receiver. Using this worst-case model we can also assess the impact of increased error propagation on the SIC receiver in high mobility scenarios.

C. *Multi-user Transmit Power Allocation*

According to (5), due to power-domain multi-user multiplexing, the transmit power allocation (TPA) to one user affects the achievable throughput of not only that user but also the throughput of other users. In order to clarify the degree of impact of user pairing and TPA on the performance of NOMA, both exhaustive and simplified user pairing and power allocation schemes are explored.

- *Full search power allocation (FSPA)*

The best performance of NOMA can be achieved by exhaustive full search of user pairs and transmit power allocations. In case of full search power allocation (FSPA), all possible combinations of power allocations are considered for each candidate user set, U_s,. FSPA remains, however, computationally complex. Also, with dynamic TPA, the signalling overhead associated with SIC decoding order and power assignment ratios increases. In NOMA, users with large channel gain difference (e.g., large path-loss difference) are paired with high probability [10]. Thus, considering practical implementations, user pairing and TPA, could be simplified. In order to clarify the impact of user pairing and TPA, the following simplified schemes are also considered.

- *Fractional transmit power allocation (FTPA)*

In order to reduce further the computational complexity, we adopt a suboptimal fractional transmit power allocation (FTPA) that is similar to the transmission power control used in the LTE uplink [7]. In the FTPC method, the transmit power of user k in candidate user set, U_s, in subband ,s ,is allocated as follows:

$$p_s(k) = \frac{P}{\sum_{j\in U_s}\left(G_s(j)/N_s(j)\right)^{-\alpha_{FTPC}}}\left(\frac{G_s(k)}{N_s(k)}\right)^{-\alpha_{FTPC}}, \qquad (6)$$

where α_{FTPC} ($0 \le \alpha_{FTPC} \le 1$) is the decay factor. The case of $\alpha_{FTPC} = 0$ corresponds to equal transmit power allocation among the users. The more α_{FTPC} is increased, the more power is allocated to the user with lower channel gain $G_s(k)/N_s(k)$. Note here that the same α_{FTPC} will be applied to all subbands and transmission times. Thus, the value of α_{FTPC} is an optimization parameter that needs to be determined *a priori* via computer simulations such that the target performance evaluation metric is maximized.

- *Pre-defined user grouping and per-group fixed power allocation (FPA)*

The users are divided into different user groups according to their channel gains and the pre-defined thresholds, denoted as Ψ in Fig. 1. In this pre-defined user grouping, the users can be paired together only if they belong to different user groups. In general, dynamic TPA according to instantaneous channel conditions of multiplexed users achieves the best performance because of its efficient utilization of the power resources. With the pre-defined user grouping, however, TPA could also be simplified by applying fixed power assignments to users belonging to the same group. For example, for the user group with good channel gain, small power (e.g. $0.2P$) is allocated and for the user group with bad channel gain, large power (e.g. $0.8P$) is allocated, where the total power assigned to different user groups is kept equal to P. Pre-defined user grouping and fixed TPA can effectively decrease the amount of downlink signalling related to NOMA. For example, the order of successive interference cancellation (SIC) and information on power assignment do not need to be transmitted in every subframe but rather on a longer time scale.

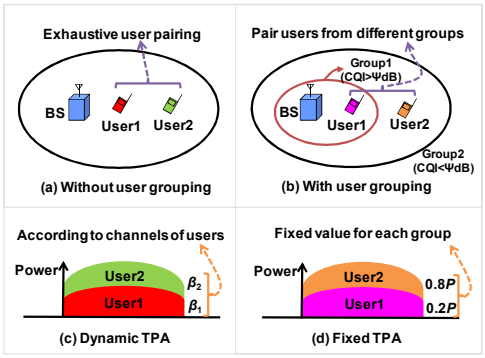

Fig. 3. User grouping and TPA for NOMA.

IV. Simulation Evaluations

A. *NOMA System-Level Simulations*

We present system-level simulation results of the investigation on the performance gains of NOMA. The simulator used consists of a system-level model utilizing exponential SINR link-to-system level mapping [14]. From all K users, after channel and interference estimation at the receiver side, the channel gain is calculated and fed back to the BS. For wideband scheduling, channel gain is a single value while for subband scheduling, channel gain consists of multiple values corresponding to different subbands. At the BS, assuming that all possible candidate user sets are searched, the number of candidate user sets is $V = \binom{K}{1} + \binom{K}{2} + \cdots + \binom{K}{m_s}$. For each subband, the scheduling metric maximizing the candidate user set is selected. The scheduling metric is calculated based on the estimated instantaneous user throughput which is derived using wideband SINR for wideband scheduling and subband SINR for subband scheduling, according to Eq. (5). Based on the SINR of each user, the MCS with the highest spectrum efficiency while satisfying targeted BLER<=0.1 is selected. At the UE side, the effective SINR is calculated for each user using EESM (exponential effective SNR mapping) model where the weighting factor beta is optimized for each MCS [14]. Based on the effective SINR, MCS decoding is attempted using the BLER vs. SINR link-level mapping table. Note that OMA follows the same procedure as NOMA but with $m_s = 1$.

B. Simulation Assumptions

To evaluate the performance gain of NOMA, a multi-cell system-level simulation is conducted. The simulation parameters are basically compliant with existing LTE/LTE-Advanced specifications [2,3]. We employed a wrap-around 19-hexagonal macrocell model with 3 cells per cell site. The cell radius of the macrocells is set to 289 m (inter-site distance (ISD) = 500 m). K UEs are dropped randomly following a uniform distribution. In the propagation model, we take into account distance-dependent path loss with a decay factor of 3.76, lognormal shadowing with the standard deviation of 8 dB, and instantaneous multipath fading. The shadowing correlation between the sites (cells) is set to 0.5 (1.0). The spatial channel model (SCM) urban macro with a low angle spread is assumed [15]. The system bandwidth is 10 MHz and the total transmission power of the BS in each cell is 46 dBm. The antenna gain at the BS and UE is 14 dBi and 0 dBi, respectively. A one-antenna transmission and two-antenna reception (1-by-2 SIMO) system is assumed and a full buffer traffic model is used. For NOMA and OMA we assume the ideal channel and intra-cell/inter-cell interference estimation and unquantized feedback of the channel gain, but with a feedback delay such that the channel gain information is not available for scheduling until 4 subframes after the periodic report with a 2 ms interval. The performance of NOMA is investigated with and without error propagation. For without error propagation, SIC perfectly removes inter-user interference. For with error propagation, the worst case model is considered as described in section III-B. The control delay of AMC is 4 ms. Table I summarizes the 23 modulation coding scheme (MCS) sets used for AMC. The simulation parameters are summarized in Table II. In order to investigate NOMA performance gains, the cell throughput and cell-edge user throughput are evaluated based on the following definitions. The cell throughput is defined as the average aggregated throughput for users scheduled per a single cell, while the cell-edge user throughput is defined as the 5% value of the cumulative distribution function (CDF) of the user throughput.

TABLE I. MCS SETS FOR AMC

Modulation Scheme	Channel Coding Rate
QPSK	1/20, 1/14, 1/10, 1/8, 1/6, 1/5, 1/4, 1/3, 2/5, 1/2, 3/5, 2/3, 3/4, 5/6
16QAM	1/2, 3/5, 2/3, 3/4, 5/6
64QAM	3/5, 2/3, 3/4, 4/5

TABLE II. MAJOR SIMULATION PARAMETERS

Cell layout	Hexagonal grid (wrap-around) 19 sites, 3 cells per site
Inter-site distance	500 m
Minimum distance between UE and cell site	35 m
Distance dependent path loss	$128.1+37.6\log_{10}(r)$ dB
Shadowing correlation	0.5(inter site)/1.0(intra site)
Channel model	3GPP Spatial Channel Model (SCM), Urban Macro
Channel estimation	Ideal
UE speed	3km/h, 20km/h, 40km/h, 60km/h, 100km/h
BS total transmission power	46 dBm
Transmit antenna gain	14 dBi
UE antenna gain	0 dBi
UE noise figure	9 dB
Thermal noise density	-174 dBm/Hz
Carrier frequency	2 GHz
System bandwidth	10 MHz
Number of transmitter antenna	1
Number of receiver antennas	2
Number of UEs per cell	K=5, 10, 20, 30
Maximum number of multiplexed UEs	1 (OMA) and 2 (NOMA)
Number of subbands	S=1 (wideband scheduling), or 8 (subband scheduling)
Scheduling algorithm	Proportional Fairness (PF)
Control delay in scheduling &AMC	4.0 ms
Channel gain reporting interval	2.0 ms
Traffic model	Full buffer model

C. Simulation Results

First, the performance gain of NOMA over OMA is investigated for S=1 (8), i.e., wideband (subband) scheduling for OMA and wideband (subband) user multiplexing for NOMA. Figure 4 provides the CDF of the user throughput for OMA and NOMA for K = 20. For NOMA, the maximum number of simultaneously multiplexed users is set to 2 and full search power allocation (FSPA) is used. It can be seen that large performance gains can be achieved by NOMA. The cell throughput gain and cell-edge throughput gain for NOMA over OMA for wideband scheduling are approximately 40% and 39% and for subband scheduling are approximately 37% and 32%, respectively. Note that for NOMA substantial gains are obtained for cell center users because they benefit more from more frequency or time resources owing to non-orthogonal user multiplexing.

Figure 4 also shows the impact of error propagation on performance of NOMA for K = 10. It can be seen that error propagation has marginal impact on NOMA performance for both wideband scheduling and subband scheduling. The reason why error propagation has marginal impact is because in most cases NOMA pairs a UE with bad channel gain (thus high transmit power) with a UE with good channel gain (thus low transmit power). As the MCS for the UE with bad channel gain is selected with a targeted BLER<=0.1, the decoding failure of data packet of the UE with bad channel gain at the UE with good channel is very small, i.e. the BLER is usually much less than 0.01. Therefore, the error propagation has marginal impact on NOMA performance.

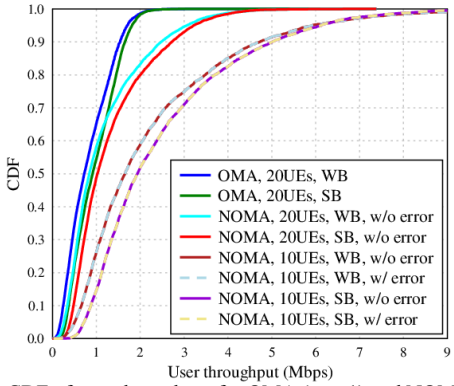

Fig. 4. CDF of user throughput for OMA (m = 1) and NOMA (m = 2) with subband and wideband scheduling.

Next, we investigate NOMA cell throughput gain with various UE speeds. Figure 5 shows the cell throughput gain of NOMA over OMA for different user speeds for wideband and subband scheduling with and without error propagation.

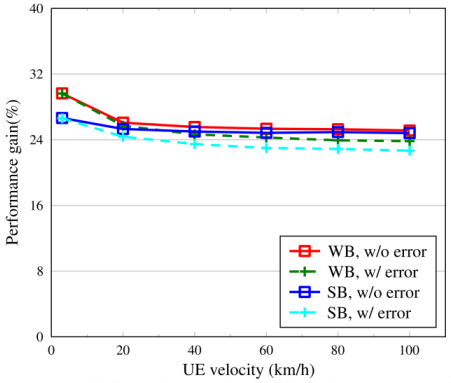

Fig. 5. NOMA cell throughput gains with various UE speeds (wideband and subband scheduling, with and without error propagation).

In Fig. 5, the number of users per cell is 10 and FTPA with α_{FTPA}=0.4 is used for NOMA power allocation. It can be seen that performance gains of NOMA over OMA are observed over a wide range of UE speeds in terms of cell throughput. Thus, NOMA provides performance gains with good robustness to mobility. The impact of error propagation is also evaluated and confirmed to be marginal for the range of UE speeds considered.

Finally, we investigate the impact of user pairing and TPA on the performance of NOMA. To this end, both exhaustive and simplified user pairing and power allocation schemes are explored. Figures 6 and 7 show the cell throughput gain and cell-edge throughput gain of NOMA over OMA for wideband scheduling with different number of users: K = 5, 10, 20, and 30.

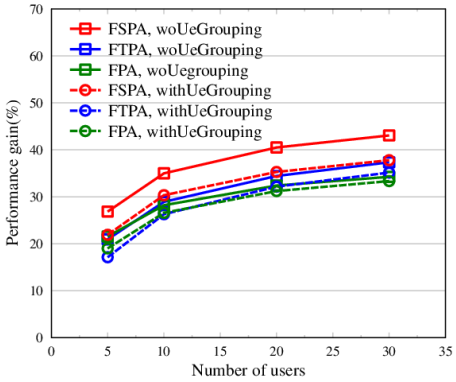

Fig. 6. NOMA gains with both full and simplified scheduling (FSPA, FTPA, FPA) (without error propagation, wideband scheduling): cell throughput.

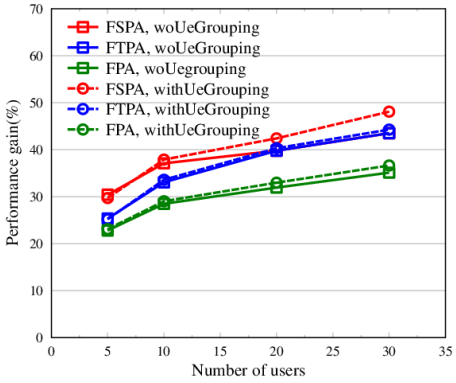

Fig. 7. NOMA gains with both full and simplified scheduling (FSPA, FTPA, FPA) (without error propagation, wideband scheduling): cell-edge throughput.

In Figs. 6 and 7, for FTPA the parameter α_{FTPA} is set to 0.5, and for FPA the threshold for pre-defined user grouping is 8 dB and the power ratio is (0.2P, 0.8P). With simplified TPA and pre-defined user grouping, a hefty portion of NOMA gains can be maintained. also note how with grouping, power allocation can be simplified with little degradation in performance. Taking into account the potential saving in signalling overhead, these simplified methods would be very promising for practical design of NOMA radio interface.

V. CONCLUSION

We evaluated the system-level performance of NOMA taking into account key aspects related to the LTE radio interface design in addition to NOMA specific functionalities such as multi-user power allocation and error propagation for SIC. Using computer simulations, we showed that the overall cell throughput and cell-edge user throughput, are all superior to those for OMA for both wideband and subband scheduling in both low and high mobility scenarios. The effect of error propagation also was shown negligibly small even in high mobility scenarios. The performance of NOMA using various user pairing and power allocation schemes was evaluated and compared. The proposed pre-defined user grouping and fixed per-group power allocation were shown able to maintain a hefty portion of NOMA gains, which is quite important to reduce downlink signalling overhead in practical interface design of NOMA for future LTE enhancements.

REFERENCES

[1] Y. Kishiyama, A. Benjebbour, H. Ishii, and T. Nakamura, "Evolution concept and candidate technologies for future steps of LTE-A," *IEEE ICCS2012*, Nov. 2012.

[2] 3GPP TS36.300, Evolved Universal Terrestrial Radio Access (E-UTRA) and Evolved Universal Terrestrial Radio Access Network (E-UTRAN); Overall description.

[3] 3GPP TR36.814 (V9.0.0), "Further advancements for E-UTRA physical layer aspects," Mar. 2010.

[4] K. Higuchi and Y. Kishiyama, "Non-orthogonal access with random beamforming and intra-beam SIC for cellular MIMO downlink," *IEICE RCS2012-89*, vol. pp. 85-90, July 2012.

[5] Y. Endo, Y. Kishiyama, and K. Higuchi, "A study on transmission power control considering inter-cell interference for non-orthogonal access with MMSE-SIC in cellular uplink," *IEICE RCS2012-46*, pp. 19-24, June 2012.

[6] J. Umehara, Y. Kishiyama, and K. Higuchi, "Enhancing user fairness in non-orthogonal access with successive interference cancellation for cellular downlink," *Proc. of ICCS*, Nov. 2012.

[7] N. Otao, Y. Kishiyama, and K. Higuchi, "Performance of non-orthogonal access with SIC in cellular downlink using proportional fair-based resource allocation," *ISWCS*, pp. 476-480, Aug. 2012.

[8] D. Tse and P. Viswanath, *Fundamentals of Wireless Communication*, Cambridge University Press, 2005.

[9] A. Benjebbour, Y. Saito, Y. Kishiyama, A. Li, A. Harada, and T. Nakamura, "Concept and practical considerations of non-orthogonal multiple access (NOMA) for future radio access," *ISPACS 2013*, Nov. 2013.

[10] Y. Saito, Y. Kishiyama, A. Benjebbour, T. Nakamura, A. Li, and K. Higuchi, "Non-orthogonal multiple access (NOMA) for future radio access," *IEEE VTC spring 2013*, June 2013.

[11] Y. Saito, A. Benjebbour, Y. Kishiyama, and T. Nakamura, "System-level performance evaluation of downlink non-orthogonal multiple access (NOMA)," *IEEE PIMRC* 2013, Sept. 2013.

[12] F. P. Kelly, A. K. Maulloo, and D. K. H. Tan, "Rate control for communication networks: shadow prices, proportional fairness and stability," *Journal of the Operational Research Society*, vol. 49, Sept. 1998.

[13] M. Kountouris and D. Gesbert, "Memory-based opportunistic multi-user beamforming," *Proc. IEEE Int. Symp. Information Theory (ISIT)*, Adelaide, Australia, Sept. 2005.

[14] K. Brueninghaus, D. Astely, T. Salzer, S. Visuri, A. Alexiou, S. Karger, and G. A. Seraji, "Link performance models for system level simulations of broadband radio access systems," *Proc. IEEE PIMRC*, Sept. 2005.

[15] 3GPP, "Physical layer aspects for Evolved UTRA," TR 25.814,V7.1.0, Oct. 2006.

ACKNOWLEDGMENT

Part of this work has been performed in the framework of the FP7 project ICT-317669 METIS, which is partly funded by the European Union. The authors would like to acknowledge the contributions of their colleagues in METIS, although the views expressed are those of the authors and do not necessarily represent the project.